23rd ABCM International Congress of Mechanical Engineering
December 6-11, 2015, Rio de Janeiro, RJ, Brazil

# HYDRAULIC TRANSIENTS IN PENSTOCKS: COMPARISON OF RESULTS OF THE SOLUTION USING RUNGE-KUTTA AND METHOD OF CHARACTERISTICS APPLIED IN THE HYDRAULIC CIRCUIT OF THE TURBINES OF THE ITAIPU POWERPLANT

**João M. Marra**
Itaipu Binacional – Av. Tancredo Neves 6731 – Foz do Iguaçu , Paraná, Brazil
*marra@itaipu.gov.br*
**Liliana M. Gramani**
Federal University of Parana – Jardim das Américas – CP 19011 – Curitiba, Paraná, Brazil
*l.gramani@gmail.com*
**Christian W. Santos**
State University of West Parana - Av. Tarquínio Joslin dos Santos 1300 – Foz do Iguaçu, Paraná, Brazil
*christianwendt.eng@gmail.com*
**Eloy Kaviski**
Federal University of Parana – Jardim das Américas – CP 19011 – Curitiba, Paraná, Brazil
*eloy.dhs@ufpr.br*

***Abstract.*** *This paper presents a comparative study of results obtained by the methods of characteristics and Runge-Kutta in the numerical solution of governing equations for determining the pressure behavior in the hydraulic system of a Francis turbine during transients in its flow. The results validation is based on available data of transients recorded during load rejection testing in the turbines of Itaipu power plant. As an application of this study is analyzed the possibility of changing the distributor's closing curve of these turbines in order to obtain a closing law which provides more favorable values of overpressure due to water hammer and overspeed in the generating unit in load rejections.*
***Keywords:*** *water hammer, penstock, turbine, hydraulic transient, numerical simulation*

## 1. INTRODUCTION

The regularization of an interconnected electrical system is a complex process and requires instantaneous and permanent action in order to equilibrate the normal oscillations and abrupt variations of load with generation, which also in its turn occur oscillations and abrupt variations, either by equipments failure or temporary loss of energetic availability of some source as, for example, the wind and solar power, which increasingly are present in the Brazilian and world energy matrix.

In this context, the hydroelectric power plants are versatile in meeting the load variations and of the interconnected power system generation, due to the rapidity in the power's response due to a favorable ratio of rotational inertia and hydraulic response. However, in meeting these variations often these plants operate outside their optimal hydraulic conditions, including due to seasonal variation in hydraulicity or hydraulic crises, increasingly frequent by global warming. In this scenario, the Francis machines, responsible for expressive contribution in the hydroelectric generation in Brazil and in the world and also for 60% of the world hydraulic potential to be installed, are normally more sensible by its intrinsic characteristics, mainly concerning the efficiency and disturbances in the flow.

The knowledge of the pressure behavior in the hydraulic system of a hydraulic turbine during flow transients is fundamental in the penstock and generating unit design stage and the correct estimate of this represents challenges due to the complexity of the actual installation of a hydroelectric plant. Although the pressure variations caused by water hammer in an abrupt load variation could be quantified with accuracy through the method of characteristics, to phenomena of resonance and hydraulic instability during normal operation of the turbine the representation of hydraulic systems through equivalent electric circuits solved by the numerical integration of Runge-Kutta presents some advantages in the mathematical modeling of the hydraulic system.

This work presents a study carried out with data from Itaipu power plant turbines using the methods of characteristics and the Runge-Kutta in the numerical simulation of pressure behavior after a load rejection, carries out a comparison with measurements available for this situation and analyses the possibility of changing the distributor closing curve of these turbines, in order to obtain a closing law which provides more favorable values of overpressure due to water hammer and overspeed in the generating unit in load rejections.

## 1. GOVERNING EQUATIONS AND ELECTRICAL ANALOGY

The hydraulic circuit of hydroelectric plants is characterized by having the much larger longitudinal dimensions than the transversal dimensions, as illustration of Fig. 1. In function of this typical configuration, the working fluid flow has predominant characteristics on longitudinal direction and negligible temperature variation, allowing a representative one-dimensional mathematical modeling of the flow dynamic behavior based on the mass and momentum conservation laws.

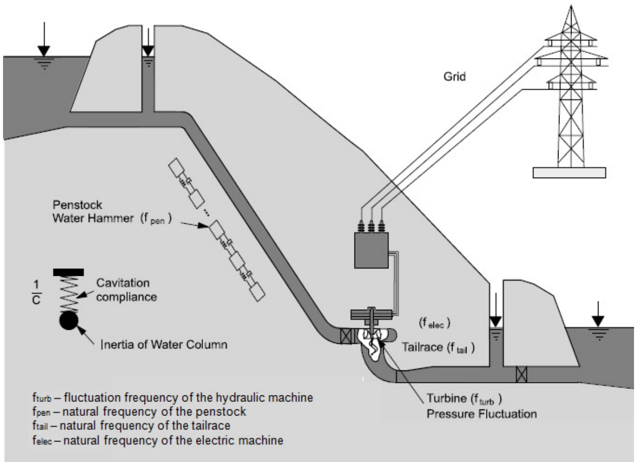


Figure 1. Scheme of typical hydraulic system of a hydroelectric plant (Adapted from IEC 60193)

According to Chaudry (2014), the application of Newton's second law on a free body diagram of forces to an elastic element of *dx* length of the tubing and continuity equation to the same element subjected to a hydraulic piezometric line results on the following governing equations system for the transient one-dimensional flow on the tubing element, where *'a'* is the celerity of the pressure waves:

$$\frac{\partial H}{\partial x}+\frac{1}{gA}\frac{\partial Q}{\partial t}+\frac{fQ|Q|}{2gDA^2}=0 \qquad (1)$$

$$\frac{\partial H}{\partial t}+\frac{a^2}{gA}\frac{\partial Q}{\partial x}=0 \qquad (2)$$

On the above system the Eq. (1) is referred to the movement equation and the Eq. (2) to a transport equation given by the mass conservation. The equations system formed is a hyperbolic first order non-linear partial differential equations system, for which the method of characteristics, based in finite differences, is traditionally used in its numerical solution for given initial and boundary conditions.

As Streeter and Wylie (1978), the equations system above is analogous to electric wave propagation in electric conductors, wherein the flow *Q* corresponds to the electric current and piezometric high *H* (or pressure) corresponds to voltage. Based on the analogy of the two systems, the parameters correspondents of the hydraulic system are qualified to traditional denominations of parameters *R* (Resistance), *L* (Inductance) and *C* (Capacitance) for an electric system, as indicated below:

$$\frac{\partial H}{\partial x}+L'\frac{\partial Q}{\partial t}+R'(Q)Q=0 \qquad (3)$$

$$\frac{\partial H}{\partial t}+\frac{1}{C'}\frac{\partial Q}{\partial x}=0 \qquad (4)$$

In the hydraulic system the parameter *R* represents the loss of energy by dissipative effects, *L* and *C* represents, respectively, the effects of inertia and storage in volume. The parameter *C* is also denominated compliance, because the storage effect is due to the fluid compressibility and the tubing elasticity. Due to the dependence of the resistance R with the flow rate *R(Q)*, the partial differential equations system (Eq. 3 and 4) is nonlinear. The apostrophe signal indicates that the values of parameters in the equations are per length unit:

$$R'=\frac{f|Q|}{2gDA^2}\left[s/m\right] \quad L'=\frac{1}{gA}\left[s^2/m^3\right] \quad C'=\frac{gA}{c^2}\left[m^2\right] \qquad (5)$$

The circuit of the hydraulic system equivalent to the electric circuit RLC is indicated on Fig. 2, where the index *i* and *i+1* represents the state variables value *(H, Q)* at the opposite ends of the element considered. The electric circuit of Fig. 2 is also representative of two segments of length *dx/2* of a line transmission with electric potential difference phase to ground respectively of $U_i$ and $U_{i+1}$ and capacitance *C* between the line and the referential of ground.

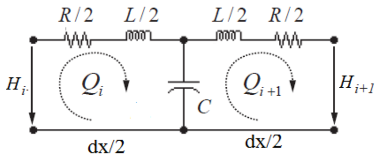


Figure 2 - Scheme of the equivalent electric circuit of the elastic tube element (Adapted from Nicolet 2007).

In function of the analogy between the hydraulic and electrical circuits, the governing equations of the hydraulic circuit can be obtained by applying the laws of Kirchoff and the law relating to electrical voltage drop (or hydraulic pressure) on the elements of the circuit, as indicated on the Tab. 1, where *I* é the current an *U* the voltage.

Table 1 – Analogy of electrical and hydraulic circuits

| Law | Application | Electric | Hydraulic |
|---|---|---|---|
| 1st Kirchhoff's law | Node law | $\sum_{i=1}^{n} I_i = 0$ | $\sum_{i=1}^{n} Q_i = 0$ |
| 2nd Kirchhoff's law | Mesh law | $\sum_{i=1}^{n} U_i = 0$ | $\sum_{i=1}^{n} H_i = 0$ |
| Ohm's law | Voltage drop on resistor | $\Delta U = RI$ | $\Delta H = RQ$ |
| Lenz's law | Voltage drop on inductor | $\Delta U = L\frac{dI}{dt}$ | $\Delta H = L\frac{dQ}{dt}$ |
| | Voltage drop on capacitor | $I = C\frac{dU}{dt}$ | $Q = C\frac{dH}{dt}$ |

## 3. SPATIAL DISCRETIZATION OF HYDRAULIC SYSTEM AND MODELING OF TUBING

In this simulation, all of the hydraulic tubing stretchs are modeled as elastics elements of steel, regardless of these being installed in apparent steel, embedded or concrete only.

### 3.1 For the runge-kutta method – RKM

For a generic pipe of length *l*, applying a discretization based in a central scheme, it can quantify the spatial variation of manometric height *H* and of flow rate *Q* at the node *i+1/2* and the mean flow value, as, respectively, expressions indicated on Eq. (6) below:

$$\left.\frac{\partial H}{\partial x}\right|_{i+1/2} = \frac{H_{i+1} - H_i}{dx} \quad ; \quad \left.\frac{\partial Q}{\partial x}\right|_{i+1/2} = \frac{Q_{i+1} - Q_i}{dx} \quad ; \quad Q_{i+1/2} = \frac{Q_{i+1} + Q_i}{2} \tag{6}$$

Figure 3 illustrates the central scheme used for spatial discretization for the f tubing lenght $l$ :

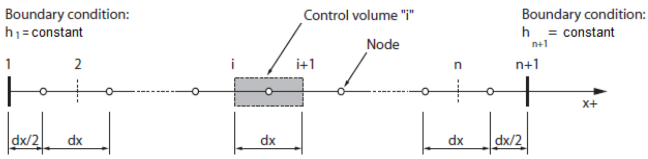


Figure 3 – One-dimensional spatial discretization of tubing (Adapted from Nicolet 2007)

For the considered elastic tube, the scheme of electric circuit equivalent to the adopted discretization is:

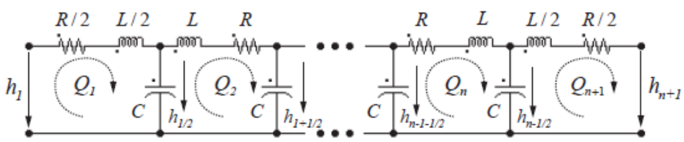


Figure 4 – Elastic tube equivalent electric circuit ( Adapted from Nicolet 2007)

Substituting the expressions of Eq. 6 in Eq. (3) and Eq. (4) and making $R'dx = R,\ L'dx = L\ e\ C'dx = C$ is obtained an ODE system for one element of elastic tube of length *dx*, that expressed in matrix form becomes:

$$\begin{pmatrix} C & 0 & 0 \\ 0 & L/2 & 0 \\ 0 & 0 & L/2 \end{pmatrix} \cdot \frac{d}{dt} \begin{pmatrix} h_{i+1/2} \\ Q_i \\ Q_{i+1} \end{pmatrix} + \begin{pmatrix} 0 & -1 & 1 \\ 1 & R/2 & 0 \\ -1 & 0 & R/2 \end{pmatrix} \begin{pmatrix} h_{i+1/2} \\ Q_i \\ Q_{i+1} \end{pmatrix} = \begin{pmatrix} 0 \\ H_i \\ -H_{i+1} \end{pmatrix} \tag{7}$$

In compact matrix form, the equation system (7) is reduced to Eq. (8), where $\vec{x} = \left(H_{i+1/2},\ Q_i,\ Q_{i+1}\right)$ is the state variables vector of the discretized system, and A and B are 3x3 matrix, becomes:

$$[A] \cdot \frac{d\vec{x}}{dt} + [B] \cdot \vec{x} = \vec{C} \tag{8}$$

For the elastic tube of length $l$ discretized as indicated on Fig 3, the matrices [A] and [B] of (Eq. 11) have order $2n+1$ and the vectors of state $\vec{x}$ (Eq. 9) and of boundary conditions $\vec{C}$ (Eq. 10) have dimension $(2n+1, 1)$:

$$\vec{x} = \left(H_{1+1/2} \quad H_{2+1/2} \quad \cdots \quad H_{n+1/2} \quad Q_1 \quad Q_1 \quad \cdots \quad Q_{n+1}\right)^T \tag{9}$$

$$\vec{C} = \left(0 \quad 0 \quad \cdots \quad H_1 \quad 0 \quad 0 \quad \cdots \quad H_{n+1}\right)^T \tag{10}$$

$$[A] = \begin{array}{c} \\ \\ \\ \\ (n) \\ \\ \\ \\ \\ (2n+1) \end{array} \begin{pmatrix} C &&&&&&&&& \\ & C &&&&&&&& \\ && \ddots &&&& 0 &&& \\ &&& C &&&&&& \\ &&&& C &&&&& \\ &&&&& L/2 &&&& \\ &&&&&& L &&& \\ & 0 &&&&&& \ddots && \\ &&&&&&&& L & \\ &&&&&&&&& L/2 \end{pmatrix}^{(2n+1)} \qquad [B] = \begin{array}{c} \\ \\ \\ \\ (n) \\ \\ \\ \\ \\ (2n+1) \end{array} \begin{pmatrix} &&&&& -1 & 1 &&& \\ &&&&&& -1 & 1 && \\ && 0 &&&&& \ddots && \\ &&&&&&& -1 & 1 & \\ &&&&&&&& -1 & 1 \\ 1 &&&&& R/2 &&&& \\ -1 & 1 &&&&& R &&& \\ & \ddots &&&&&& \ddots && \\ &&& -1 & 1 &&&& R & \\ &&&& -1 &&&&& R/2 \end{pmatrix}^{(2n+1)} \tag{11}$$

### 3.2 For the method of characteristics – MOC

The method of characteristics can be used widely to solve initial value problem relative to first order ODE and that when applied to a PDE with tow variables the change of coordinates of the process transforms the PDE in ODE along certain curves called characteristic curves, over which the new variables will be disclosed in the characteristic curves (Sarra, 2003). The application of the method of characteristics on the governing equations (1) and (2) results in two ODE systems (Eq. 12) correspondents to two characteristics equations relatives to the propagation of the wave flow direction (positive) and on opposite direction (negative). According to Streeter and Wylie (1978), such systems of equations are:

$$\begin{cases} \dfrac{dH}{dt} + \dfrac{a}{g.A}\dfrac{dQ}{dt} + \dfrac{a}{g}\dfrac{f.Q.|Q|}{2.D.A^2} = 0 \\ \dfrac{dx}{dt} = +a \end{cases} \qquad \begin{cases} \dfrac{dH}{dt} - \dfrac{a}{g.A}\dfrac{dQ}{dt} - \dfrac{a}{g}\dfrac{f.Q.|Q|}{2.D.A^2} = 0 \\ \dfrac{dx}{dt} = -a \end{cases} \tag{12}$$

The spatial discretization of the hydraulic system and the spatial-temporal adopted for the method of characteristics are respectively illustrated in Fig. 5.a and Fig. 5.b. On this process, waves travel with the celerity $a$ along the characteristic lines, represented on the plane (x, t) by diagonals lines, obeying to the relationship $a = \Delta x / \Delta t$ .

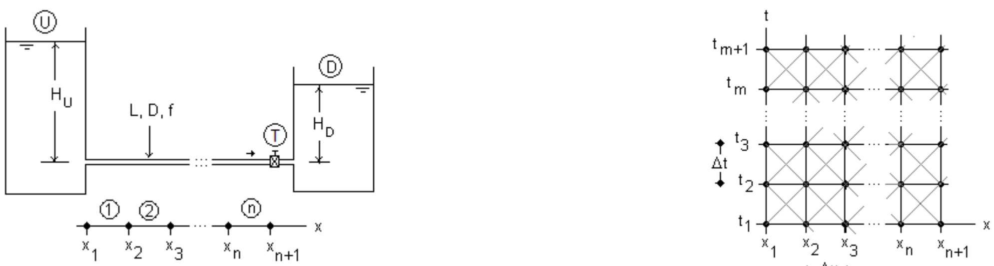


Figure 5 – a) Spatial discretization of hydraulic; b) Spatial and temporal discretization

According to Urroz (2004), applying progressive finite differences to the derivatives of equations (12) and integrating over the positive characteristic lines (CP) and negatives ones (CN) is obtained the expressions of Eq. (13) where $B = (a/g.A)$ and $R = f/(2.g.D.A^2)$:

$$\begin{cases} H_i^{j+1} + B.Q_i^{j+1} = H_{i-1}^j + B.Q_{i-1}^j - R.Q_{i-1}^j.\left|Q_{i-1}^j\right|(\Delta x) = CP \\ H_i^{j+1} - B.Q_i^{j+1} = H_{i+1}^j - B.Q_{i+1}^j + R.Q_{i+1}^j.\left|Q_{i+1}^j\right|(\Delta x) = CN \end{cases} \tag{13}$$

By solving the linear system represented by Eq. (13), is obtained the expression of Eq. (15) that quantifies respectively the amplitudes of pressure and flow rate in the hydraulic system in the discretized domain:

$$H_i^{(j+1)} = (CP + CN)/2 \qquad Q_i^{(j+1)} = (CP + CN)/(2.B) \tag{14}$$

## 4. MODELING OF HYDRAULIC SYSTEM

This section discusses the geometric modeling the variation of the diameter of the pipe along the hydraulic system from the water to the outlet end of the spiral casing and also the modeling of the functional elements which were considered as concentrates (lumped), so shaft surge tank and turbine distributor of the turbines of ITAIPU (Fig. 5.a).

### 4.1 Tubing

The variation of the pipe diameter at the input stream, the upper curve, straight stretch, lower curve and spiral casing hydraulic turbines of ITAIPU is shown in Fig. 6.b.

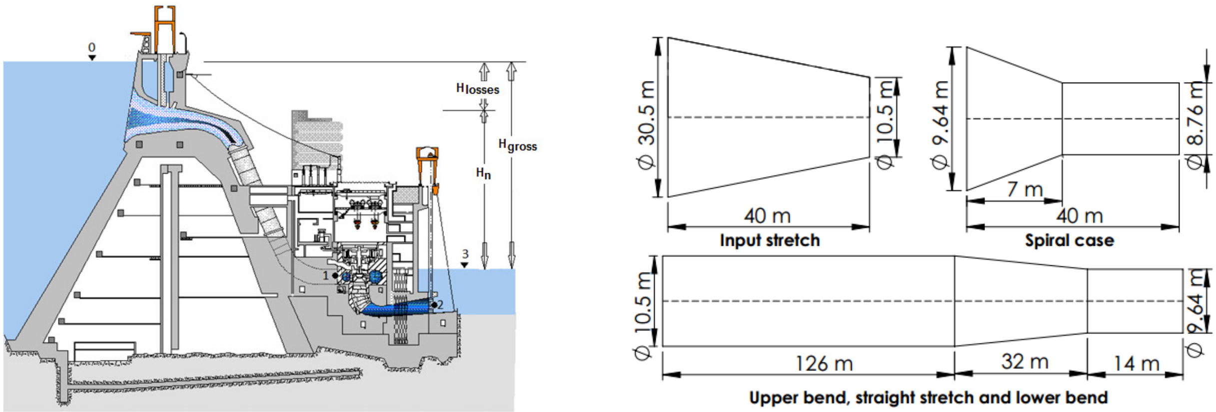

Figure 6 – a) Hydraulic system; b) Geometric modeling

The coefficient of friction in hydraulic surfaces was obtained from data available of pressure drop in the hydraulic system and Darcy-Wisbach equation, resulting in an average value of 0.025.

### 4.2 Shaft surge tank

The duct to purging of atmospheric air in the turbine and penstock priming and the gate and the stop-log's niche existing on the hydraulic system of the input stretch work as small surge tank during transients of the normal operation or load rejection. The adopted mathematical model for the element on RKM and MOC was as indicated on Fig. 7.a and Fig. 7.b, respectively as Nicolet (2007) and Chaudry (2012).

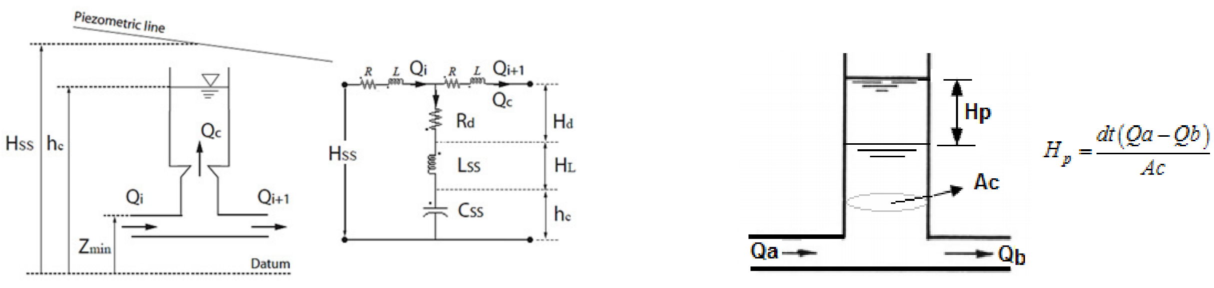

Figure 7 – Mathematical model of the shaft surge tank a) RKM; b) MOC

Solving the circuit, obtains the Eq. (15) compatible with the discretization and state vector adopted in the application of Runge-Kutta for this element of the hydraulic system:

$$\begin{bmatrix} C_{ss} & 0 & 0 \\ 0 & (L+L_{ss}) & -L_{ss} \\ 0 & -L_{ss} & (L+L_{ss}) \end{bmatrix} \cdot \frac{d}{dt}\begin{bmatrix} h_c \\ Q_i \\ Q_{i+1} \end{bmatrix} + \begin{bmatrix} 0 & -1 & 1 \\ -1 & (R+R_d) & -R_d \\ 1 & -R_d & ((R+R_d)) \end{bmatrix} \cdot \begin{bmatrix} h_c \\ Q_i \\ Q_{i+1} \end{bmatrix} = \begin{bmatrix} 0 \\ H_{ss} \\ -h_{i+1} \end{bmatrix} \tag{15}$$

In the case of the method of characteristics, the modeling used for the ventilation duct was only based on the continuity equation, resulting in the equation indicated in the illustration of Fig. 6.b.

### 4.3 Wicket gate

The flow curve in function of the free area of the turbine distributor $A_W$ , under static condition, was modeled based on the determination of the discharge coefficient $C_D$ from data of absolute measurement and net head $H_n$ avaible in Itaipu (2008) e Itaipu (2006-a), using the relation of Eq (16):

$$Q_W = C_D.A_W\sqrt{2g.H_n} \tag{16}$$

For dynamic condition, the curve of flow in the distributor during an abrupt closure was modeled based on the temporal law dispenser closure, where $b$ is the height of the vanes, and the opening $S$, as the relationship of Eq. (17):

$$Q_t = C_D.A_t\sqrt{2g.H_n} = C_D.(24\cdot b\cdot S)\sqrt{2g.H_n} \tag{17}$$

The curves for the discharge coefficient, closing law and flow curve in the distributor are shown in Fig. 8:

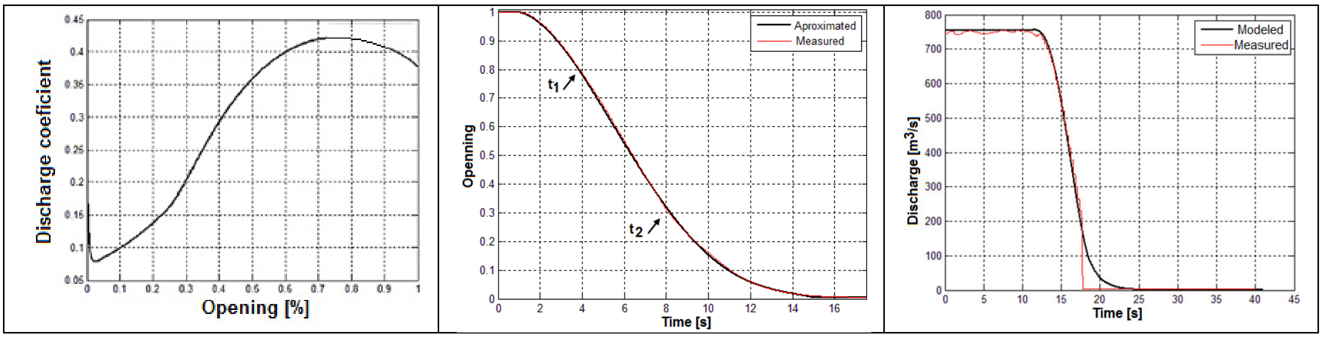


Figure 8 – a) Discharge coefficient;  b) Closing Law;  c) Flow curve

In order to facilitate the analysis of the influence of the variation of closure law in overpressure and in overspeed, it was modeled considering the possibility of changing the closing time by changing the opening in $t_1$ and opening and time in $t_2$ for a given distributor initial opening in $t_o$ . The initial stretch of curve of the Fig. 8.b was modeled by a polynomial, the intermediate stretch by a straight and the final stretch by an exponential. The flow curve of Fig. 8.c refers to the studied case with initial flow of 745 $m^3/s$, considered as the maximum possible (100%) according to the hill curve of ITAIPU turbines.

### 4.4 Rotating parts

The sudden load rejection of a generating unit for decoupling thereof with the electrical system provides an unbalancing of torque between the turbine and generator, and a consequent increase in speed. Because of this, the turbine speed governor commands the closing of the turbine distributor, which in turn causes a transient hydraulic pressure in the penstock, known as water hammer. In this condition, assuming that the magnetic torque in the air gap torque in the generator cancels instantly, the rotation speed $N$ of the rotating assembly becomes dominated by the mechanical torque $T_{mec}$ and the rotational inertia $J$, according to Eq. (18):

$$T_{mec} - T_{mag} = \left(\frac{2\pi}{60}\right) J \frac{dN}{dt} \tag{18}$$

Equation 18 can be integrated by separation of variables, whose discrete approximation of the solution given by Eq. (20) allows for the evolution of turnover during the transient from the power rejected the turbine at rated speed. During the transient, the shaft power of the turbine was evaluated by the expression: $P = \gamma Q_t H_n \eta$ . The moment of inertia was achieved by existing measurements of $GD^2$ factor, whose value was considered 363950 $tm^2$, equivalent to a moment of inertia 9.275E6 kg $m^2$.

$$N_{t+1} = \sqrt{N_t^2 + \left(\frac{60}{2\pi}\right)^2 \frac{\Delta t}{J}\left(\left(P_{t+1}+P_t\right)-P_b\right)} \tag{19}$$

Stopping power was obtained by assuming the permanence of losses dependent on voltage generator (2.1 MW) and the variation of friction losses (2.1 MW) in the bearings and ventilation proportional to the cube of change in rotation.

## 5. RESULTS

The comparative study performed in this study was based on measurements available at Itaipu (2006 .b) relative to a load rejection of 785MW, with full opening of the distributor and gross head of 120.2 mca. Considering the losses in the generator, as Itaipu (2008.b), the rejected power in the turbine shaft was estimated in 794MW, corresponding to flow of 745 m3/s and net head of 118.4 mca by the hill curve of the turbine. In numerical simulations of this condition by the methods RKM and MOC the minimum time interval in computational iterations has respected the criteria Courant-Friedrich-Levy, which establishes that the Courant number $Cr = a \cdot \Delta t / \Delta x = a \cdot n \cdot \Delta t / l$ must lower or equal the unit. In Table 2 are indicated the parameters of simulation for both methods and the percentage difference from the measured value for the overpressure and overspeed:

Table 2 – Parameters of simulation

| Method | $l$ [m] | n | a [m/s] | $\Delta$t [s] | Cr | f | Simulated time [s] | Simulation time [h] | ΔP [%] | ΔN [%] |
|---|---|---|---|---|---|---|---|---|---|---|
| Runge-Kutta | 252 | 200 | 1115 | 5.83e-5 | 0.05 | 0.025 | 40 | 12,33 | 0,41 | 0,84 |
| Characteristics | 252 | 1800 | 1115 | 1.25e-4 | 1 | 0.025 | 40 | 10,05h | 0,93 | -0,48 |

The time evolution of the pressure obtained by the methods RKM and MOC is indicated on Fig. 9.a and 9.b. The maximum values for overpressure $\Delta P$ and overspeed $\Delta N$ by both methods are equivalent and acceding to the values measured. Both methods also captured the reduction of the pressure immediately after the start of the transient and also the overlap of positive and negative waves in the pressure, marked by period $T = 4L/a =$ 0,735s and corresponding frequency of 1.36 Hz. The slight reduction in pressure before its rise can be attributed to the inertia of the flow, providing an increase in speed energy at the beginning of the distributor closure.

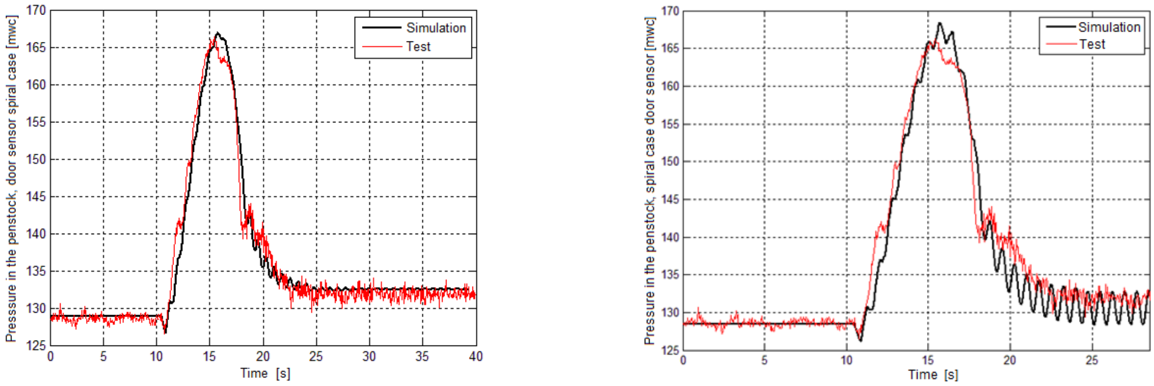


Figura 9 – a) Pressure by Runge-Kutta method; b) Pressure by method of characteristics

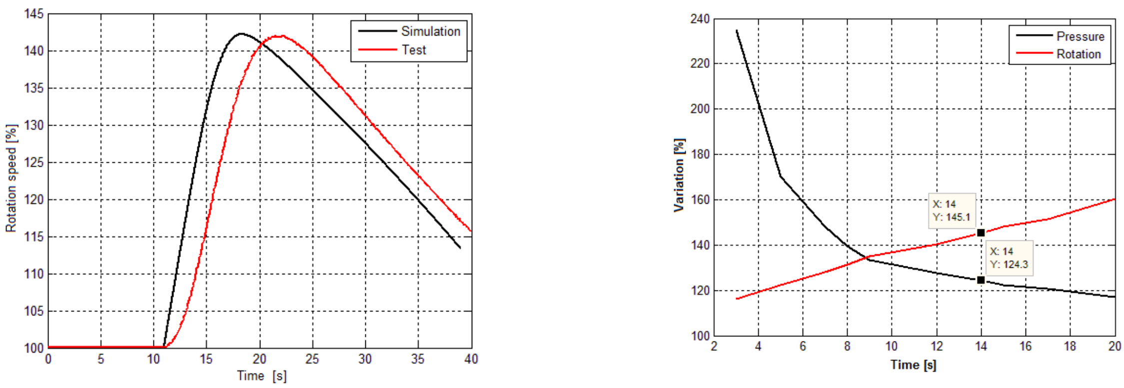


Figura 10 – a) Overspeed; b) Closing Time x overpressure and maximum overspeed

The simulation by MOC has presented numerical instability. In order to avoid that this phenomenon affects the evaluation of the maximum pressure, we opted to work with the maximum Courant in this method. However, the increase of the oscillation amplitude after approximately the simulation time 19 s is due to this phenomenon. See Fig. 9.b.

The overspeed curve of Fig. 10 may be considered equivalent for both methods, since the overpressure curves were also similar. The abrupt acceleration of the rotation at the simulated transient beginning is due to the consideration of instant interruption of the magnetic torque. The time lag between measured and simulated values can be attributed mainly to the lack of updating the turbine efficiency with the variation of rotation.

The results of the simulations with variation in the closure law are shown in Fig. 10.b, in which is evidenced the possibility of reducing approximately 7% in overspeed, keeping the nominal limit of 30% in overpressure.

## 6. CONCLUSION

The overpressure and overspeed for a given rejection is directly affected by the distributor closing law and the numerical simulation of these phenomon in hydraulic transients allows to assess in the design phase the closing law and rotational inertia necessary to meet the contracted values for the same.

The application of computer simulation of hydraulic transient and overspeed in existing generating units allows reassess the possibility of changing the closing law to obtain a more advantageous closing law and avoiding perform such study experimentally.

The solution of the transient by Runge-Kutta method presents good adhesion of results and has not presented numerical instability for any spatial discretization, while the MOC demanded greater discretization, possibly due to the type of element of elastic tube used be of constant section.

## 7. LIST OF SYMBOLS

A [$m^2$] – cross section of pipe
Aw [$m^2$] – free static area of the distributor
At [$m^2$] – free dynamic area of the distributor
C [$m^3$] – capacitance
D [m] – diameter
H [mca] – piezometric head
Hn [mca] – net head
J [kg $m^2$] – moment of inertia
L [$s^2/m^2$] – inductance
N [rpm] – rotation
Q [$m^3/s$] – discharge
R [s] – resistance
S [m] – vane opening
Z [m] – height

a [m/s] – wave celerity
b m] – vane height
x [m] – longitudinal position
t [s] – time
f – friction factor
g [$m/s^2$] – acceleration of gravity
$l$ [m] – length
η – turbine efficiency
$\gamma$ [$N/m^3$] - specific weight of water

## 8. REFERENCES

Chaudry, M. H., 2014. *Applied Hydraulic Transients*. Springer, 3rd edition.
Itaipu, 1992, Technical Report, Acceptance tests in an explanatory way – Itaipu Binacional, Brazil.
Itaipu , 2006.a. Technical Report, Hydraulic stability test – Comissioning of the U9A. Itaipu Binacional, Brazil.
Itaipu , 2006.b. Technical Report, Load rejection test – Comissioning of the U9A. Itaipu Binacional, Brazil.
Itaipu , 2008.a. Technical Report, Determination of the efficiency of the turbine U18A. Itaipu Binacional, Brazil.
Itaipu, 2008.b. Technical Report, Determination of the efficiency of the generator U18A. Itaipu Binacional, Brazil.
Nicolet, C.,*2007. Hydroacoustic Modelling And Numerical Simulation Of Unsteady Operation Of Hydroelectric Systems*. 334 p. Tese (Doutorado) - Escola Politécnica Federal de Lausana, Lausana, Suíca.
Sarra, S. A., 2003. "The Method of Characteristics with applications to Conservation Laws**.** " *Journal of Online Mathematics and its Applications*, Vol. 3.
Streeter, V.; Wylie, E., 1978 *Fluid Transients*. McGraw-Hill Inc.
Urroz, G. E., 2004. Hydraulic pipe transients by the the method of characteristics. 20 Mar. 2015.
< http://twixar.me/0H5>.

## 9. RESPONSIBILITY NOTICE

The authors are the only responsibles for the printed material included in this paper.